RESEARCH PAPER

Electrochemical Preparation and Characterization of Mn_5O_8 Nanostructures

Mustafa Aghazadeh

Materials and Nuclear Research School, Nuclear Science and Technology Research Institute (NSTRI), Tehran, Iran

ARTICLE INFO

Article History:
Received 12 October 2017
Accepted 05 December 2017
Published 01 January 2018

Keywords:
Heat-treatment
Mn_5O_8 nanorods
Pulse electrodeposition

ABSTRACT

Electrochemical synthesis followed by heat-treatment is a facile and easy method for preparation of nanostructured metal oxides. Herein we report nanostructured Mn_5O_8 prepared through pulse cathodic deposition followed by heat-treatment for the first time. For the preparation of Mn_5O_8 nanorods, pulse cathodic electrodeposition was first done from 0.005M $Mn(NO_3)_2$ at the current density of 5 mA cm^{-2} which yield Mn_3O_4 precursor. Then, heat-treatment of the deposited precursor was performed to obtain final Mn_5O_8 product. The structural and morphological properties of the prepared product were investigated by XRD, FT-IR, SEM and TEM techniques. The analysis results revealed that the prepared sample has pure Mn_5O_8 composition with rod morphology at nanoscale. Mechanism of deposit formation during pulse deposition was proposed and discussed. The formation of Mn_5O_8 nanorods via calcination of Mn_3O_4 precursor was also studied by thermogravimetric analysis. The results suggested that the cathodic electrodeposition-heat treatment method can be considered as simple and facile route for preparation of Mn_5O_8 nanorods.

How to cite this article
Aghazadeh M. Electrochemical Preparation and Characterization of Mn_5O_8 Nanostructures. J Nanostruct, 2018; 8(1): 67-74.
DOI: 10.22052/JNS.2018.01.008

INTRODUCTION

Nowadays, nanostructured Mn oxides have attracted considerable interests due to their characteristic physical and chemical properties. Such properties strongly depends on the size, shape, and dimensions, which are the important key factors necessary for the ultimate performance towards enormous potential applications in the fields of catalysts [1], magnetism [2], energy conversion and storage devices i.e. batteries [3] and supercapacitors [4].

Mn oxides (MnO, Mn_2O_3, Mn_3O_4, Mn_5O_8 and MnO_2) have typically tunnel- and/or layered-crystal structures with varied proportions of Mn at different oxidation states (2+, 3+ and 4+). The layered Mn oxides contain two-dimensional (2D) infinite elemental sheets of edge shared MnO_6 octahedrons and interlayer species. The structures and properties of these Mn oxides can be easily modified by the engineering of the interlayer and/or intralayer species, which results new material systems with novel properties and applications. In addition to the birnessite-type Mn oxides, which have layered structures, it has been reported that Mn_5O_8 also forms layered structures [5–7]. This compound was first prepared by Klingsberg and Roy via the solid-solid and solid-vapor reactions in the Mn-O system [5]. Mn_5O_8 has a isostructure with monoclinic $Cd_2Mn_3O_8$ determined by Oswald et al. [6,7] and a compositional formula of $Mn_2^{2+}Mn_3^{4+}O$. Due to its special characteristics, like mixed valence nature (i.e., Mn^{2+} and Mn^{4+}) and the interlayer and/or interlayer defects, Mn_5O_8 can display specific properties that are uncommon in

* *Corresponding Author Email: maghazadeh@aeoi.org.ir*

other mixed valence Mn oxides and/or layered materials. Notably, mixed valence states and the antiferromagnetic nature of Mn_5O_8 nanoparticles change them to a promising material for different applications such as magnetic thin-film devices, hard-disk sensors, magnetic random access memories, magneto-logic devices, etc [8,9]. For example, Mn_5O_8 nanoparticles have an antiferromagnetic behavior, which is due to the presence of two types of Mn valencies (Mn^{2+} and Mn^{4+}) that possess different types of magnetic moments [8,9]. Mn_5O_8 further enjoys excellent ion transport capabilities, which results from the interlayer and/or intralayer defects. This capability motivates its use as an ionic conductor for fuel cells or batteries. Moreover, the mixed valence nature of Mn_5O_8 makes a promising candidate for catalyst applications [10].

Until now, it has been reported that Mn_5O_8 can be prepared via chemical routes like as precipitation, sol-gel, hydrothermal and solvothermal procedures followed by calcination [11-17]. For example, Gao et al. [11] prepared Mn_5O_8 nanorods by a topotactic conversion of γ-MnOOH nanorod precursors in nitrogen at 400 °C. They showed that the prepared Mn_5O_8 nanorods are antiferromagnet with a Neel temperature of about 133 K through magnetic measurements. Park and Deoff [12] synthesized Mn_3O_4, Mn_5O_8 and α-Mn_2O_3 nanoparticles by calcination of Mn(II) glycolate nanoparticles obtained through a polyol route. They investigated time- and temperature-dependent phase transformations occurring during oxidation of the Mn(II) glycolate precursor to the different manganese oxides species (i.e. α-Mn_2O_3, Mn_3O_4 and Mn_5O_8) in O_2 atmosphere by in situ X-ray diffraction (XRD) measurements. Punnoose et al. [13] reported the Mn_5O_8 preparation with crystallite size 14 nm thought reacting manganese nitrate and sodium hydroxide at pH 12 and heating the product at 400 °C for 3 h. They also confirmed the antiferromagnetism characteristics of prepared nanocrystals by measuring the temperature variations of the magnetic susceptibility and the electron spin resonance. Sugawara et al. [14] reported a novel route for preparation of Mn_5O_8 via decomposition of citrate precursor obtained through reaction of manganese nitrate and citric acid. The following decomposition process was proposed for the Mn_5O_8 formation in air and O_2 atmosphere, respectively [14]:

$$\text{citrate precursor} \xrightarrow{\approx 250\,^{\circ}C} Mn_3O_4 \xrightarrow{>500\,^{\circ}C} Mn_2O_3 \quad \text{in air}$$

$$\text{citrate precursor} \xrightarrow{\approx 250\,^{\circ}C} Mn_3O_4 \xrightarrow{300-400\,^{\circ}C} Mn_5O_8 \xrightarrow{>500\,^{\circ}C} Mn_2O_3 \quad \text{in } O_2$$

Fritsch et al. [16] reported that the oxidation of hausmannite (Mn_3O_4) at low temperatures (300°C <T <425°C) lead to formation of Mn_5O_8. They observed that both Mn^{2+} and Mn^{3+} cations are oxidized in this temperature range, where oxidation of Mn^{2+} to Mn^{3+} is governed by a diffusion process and α-Mn_2O_3 is obtained, and oxidation of Mn^{3+} to Mn^{4+} results the crystalline Mn_5O_8 phase. Recently, the biosynthesis of Mn_5O_8 nanoparticles in the size range of 10–11 nm at room temperature has been performed through challenging the fungus Fusarium oxysporum with manganese (II) acetate tetrahydrate [$(CH_3CO_2)_2Mn\cdot 4H_2O$] as precursor [17]. Notably, all the mentioned research have emphasized that an additional calcination step is vital to obtaining a pure Mn_5O_8 phase [11-17]. An advantage of the calcination route is the conservation of the morphology and size of the precursor during this process. Although, it has been reported that chemical routes yield Mn_5O_8 species at the nanometer scale, they necessitate long reaction times, subsequent drying processes and in some cases result mixed Mn oxides (e.g. Mn_5O_8 and Mn_2O_3 [11-16]). In this area, electrochemical route (i.e., cathodic electrodeposition) has proven to be a versatile and controllable technique for preparation of nanostructured hydroxides and oxides [18-24]. In this technique, metal hydroxide as a precursor is prepared by electrodeposition process and then converted into the metal oxide via heat-treatment. The structure, morphology and uniformity of the products can be controlled by adjusting the electrodeposition parameters such as deposition mode and time, applied potential, current density, bath temperature, electrolyte concentration and additive agents [19]. However, electrochemical routes have been not applied to prepare Mn_5O_8 and there is no report on the electrochemical preparation of Mn_5O_8. The nanostructured Mn_5O_8 has also been rarely reported and only two reports based on the chemical routes are available in literature [11,17]. So, the preparation of Mn_5O_8 through electrochemical deposition route can be regarded as an interesting, yet unexplored area of research. Herein we report a novel preparation method of nanostructured Mn_5O_8 i.e. cathodic deposition followed by heat-treatment. In this two-step method, the precursor was firstly deposited on the cathode surface via base (OH^-) electrogeneration and then was heat-treated to obtain the final oxide

product. The prepared Mn_5O_8 was characterized by XRD, IR, TG and SEM techniques.

MATERIALS AND METHODS

Preparation of Mn_5O_8

Mn_3O_4 precursor was prepared via a one-step process, including the cathodically electrodepositing from nitrate bath at a pulse current (PC) mode in a typical on-times and off-times (t_{on}=5 ms and t_{off}=5 ms) with a peak current density of 5 mA cm^{-2} (I_a= 5 mA cm^{-2}). An aqueous solution of 0.005 M $Mn(NO_3)_2$ was used as deposition bath. The deposition time and bath temperature were 30 min and 25 °C, respectively. Prior to each deposition, the steel substrates were given a galvanostatically electropolishing treatment. The deposition experiments were conducted using an electrochemical workstation system (Potentiostat/Galvanostat, Model: NCF-PGS 2012, Iran). After the deposition, the steel substrates were repeatedly rinsed with water and then dried at 50 °C for 1h. Finally the deposits were scraped from the substrate and subjected to further analyses. To obtain oxide product, the prepared powder was heat treated at 400°C for 2h in O_2 atmosphere.

Characterization

The phase composition and structure of the prepared samples were investigated by powder X-ray diffraction (XRD), which was recorded on a Phillips PW-1800 diffractometer with a Cu Kα radiation source in 2θ values ranging from 10 to 70° with a scanning rate of 5 degree/min. FTIR spectra of the samples were obtained using a Bruker Vector 22 Fourier transformed infrared spectroscopy with samples in a KBr wafer at ambient temperature. Each FTIR spectrum was acquired after 20 scans at a resolution of 4 cm^{-1} from 400 to 4000 cm^{-1}. The morphologies of the prepared Mn_3O_4 and Mn_5O_8 powders were studied using a scanning electron microscope (SEM, LEO 1455 VP, Oxford, UK, operating voltage 30 kV). Transmission electron microscopy (TEM) images were also acquired using a Phillips EM 208 transmission electron microscope with an accelerating voltage of 100 kV. Thermogravimetric analysis (TGA) and differential scanning calorimetric (DSC) analysis were carried out in air between room temperature and 400°C at a heating rate of 5°C min^{-1} using a thermoanalyzer (STA-1500).

RESULTS AND DISCUSSION

Structural characterizations

The crystal structure of the prepared samples was evaluated by XRD which are shown in Fig. 1. The XRD pattern of the deposited sample is shown in Fig. 1a. All peaks of this pattern can be well indexed to hausmannite i.e. Mn_3O_4. In fact as seen in Fig. 1, all peaks of the XRD pattern of deposited sample are completely consist with Mn_3O_4 reference data (JCPDS No. 024-0734). The

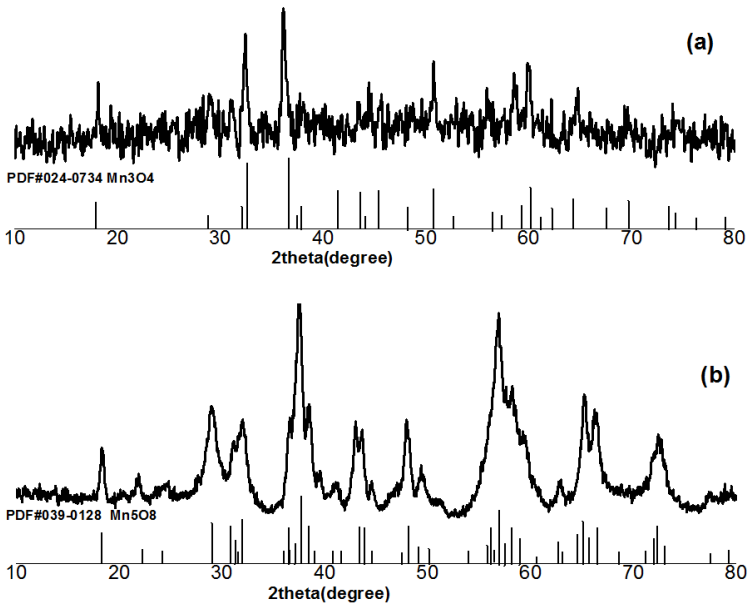

Fig. 1. XRD patterns of electrodeposited and calcined products.

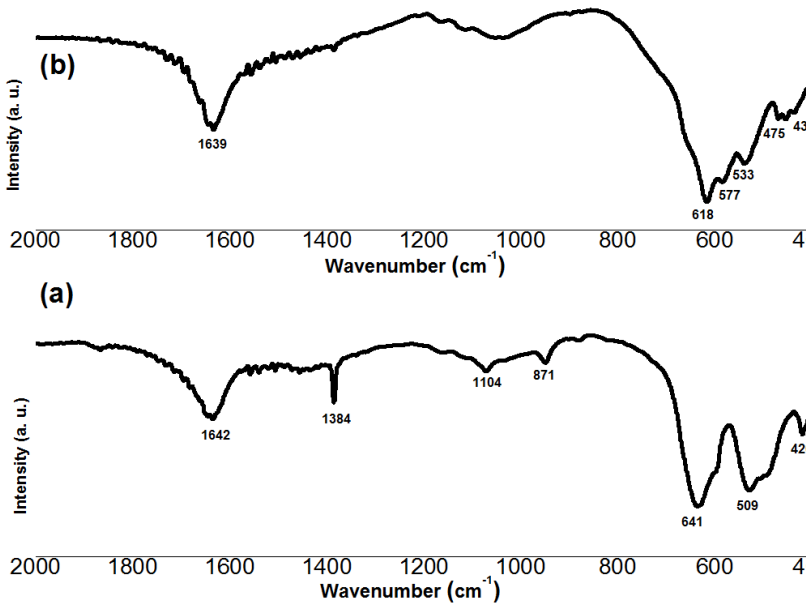

Fig. 2. FT-IR spectra of the prepared Mn_5O_8 and Mn_5O_8 products

XRD pattern of the calcined sample is shown in Fig. 1b. As can be seen, the calcined sample show well defined Bragg's reflections indicating its crystalline nature. XRD pattern of the calcined sample clearly indicates that the observed diffraction peaks are in good agreement with the monoclinic phase of Mn_5O_8 (JCPDS 39-1218, C2/m, a=10.34 Å, b = 5.72 Å, c=4.85 Å, β =109.4°). Also, the peaks have broadened characteristic indicating small crystalline size of the obtained Mn_5O_8. Futhermore, no other phase of manganese oxide (i.e. Mn_3O_4) is observed in Fig. 1b indicating the complete conversion of the Mn_3O_4 precursor to Mn_5O_8 during the calcination process. In order to gain more information on the prepared samples, FT-IR evaluations were carried out in the wavelength range of 400-2000 cm^{-1}. Fig. 2 illustrates the FT-IR spectra of the prepared samples. For the electrodeposited sample (i.e. Mn_3O_4), several absorption bands were observed at 1642, 1384, 1104, 871, 641, 509 and 426 cm^{-1} (Fig. 2b). The band at 1642 cm^{-1} are usually attributed to bending vibrations of –OH combined with Mn atoms [25,26]. Generally, the peaks in the range of 400-1000 cm^{-1} are indicative of the existence of octahedral MnO6 [27-29]. The peak located at 654 cm^{-1} is characteristic of Mn–O stretching modes in tetrahedral sites, whereas the vibration frequency located at 524 cm^{-1} corresponds to the distortion vibration of Mn–O in an octahedral environment [29]. The third vibration band, located at 417 cm^{-1}, can be attributed to the vibration of manganese species (Mn^{3+}–O) in the octahedral site of Mn_3O_4 [28-30]. The FT-IR pattern of Mn_5O_8 in Fig. 2b exhibits several distinctive peaks in the range of 400-700 cm^{-1}. These peaks are located at 618, 577, 533, 475 and 431 cm^{-1}. There is no enough information about IR spectrum of Mn_5O_8 in the literature; however, the observed peaks are completely in agreement with the peaks observed in Raman spectrum of Mn_5O_8 reported by Azzoni et al. [31].

Morphological characterization

Morphological characteristic of the prepared product was investigated by SEM and TEM. Fig. 3a shows the SEM observation of the prepared Mn_5O_8. The SEM images showed that the prepared sample has rod-like morphology at nanoscale. Notably, some of the observed rods are stacked with each other and has no special growth direction. It is also obvious that the prepared nanorods are partly uniform in size. High magnification by TEM (in Fig. 3b) revealed that the prepared nanorods are approximately 50 nm in dimeter and their length reach up to several ten nanometers. Energy dispersive spectroscopy (EDS) analysis (Fig. 3c) indicates that only Mn and O are present, which confirmed the purity of the prepared product.

Mechanism of Mn_3O_4 precursor formation

Formation of the Mn_3O_4 deposit on the cathode

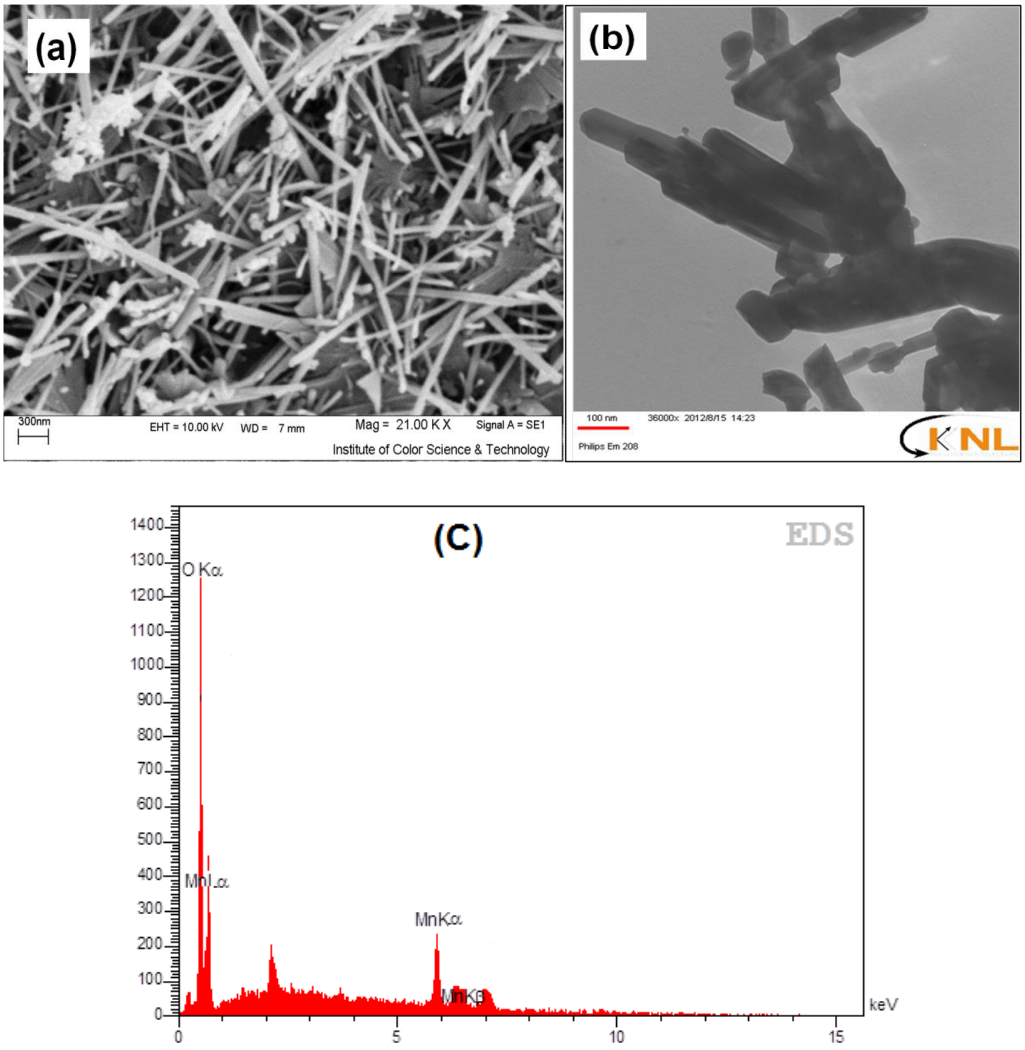

Fig. 3. (a) SEM, (b) TEM images and (c) EDS pattern of the prepared Mn_5O_8 product

surface from the nitrate bath can be explained on the bases of a two–step electrochemical–chemical (EC) mechanism [26,27] as graphically shown in Fig 4.

- The Electrochemical step:

$$2H_2O + 2e^- \rightarrow H_2 + 2OH^- \quad E^o = -1.08\ V \quad vs.\ Ag/AgCl$$

The above reactions result in an increase of the pH near the steel electrode surface. By increasing the OH^- concentration, Mn_3O_4 will form and deposit on the cathode electrode:

- The Chemical step:

$$3Mn^{3+}(aq) + 6OH^-(aq) + 1/2O_2 \rightarrow Mn_3O_4 + 3H_2O$$

Notably, considering the value of the observed potential (-1.09 V vs. Ag/AgCl) during the deposition process, it is expected that the reduction of water (Eq. (3)) has a major role in the electrogeneration of base at the applied current density. In fact, the electrochemical step is preceded by reaction (3) during the deposition process as schematically shown in Fig. 4a. The flow of gas bubbles was observable on the cathode surface throughout the deposition step, which confirmed the electrogeneration of a base as a result of the electrolysis of water. The H_2 gas bubbles can also affect the surface morphology of the hydroxide deposit and also act as a dynamic template for the formation and the growth of deposit [32,33]. A graphically shown in Fig. 4a, water molecules are reduced in the electrochemical step, and OH^- ions and H_2 molecules are produced on the cathode

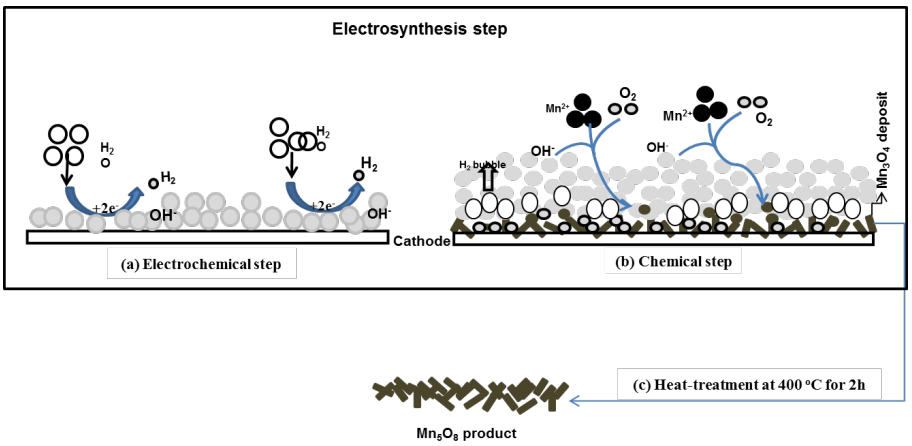

Fig. 4. Schematic view of Mn_5O_8 formation by electrosynthesis-calcination method; (a) electrochemical (b) chemical and (c) heat-treatment steps.

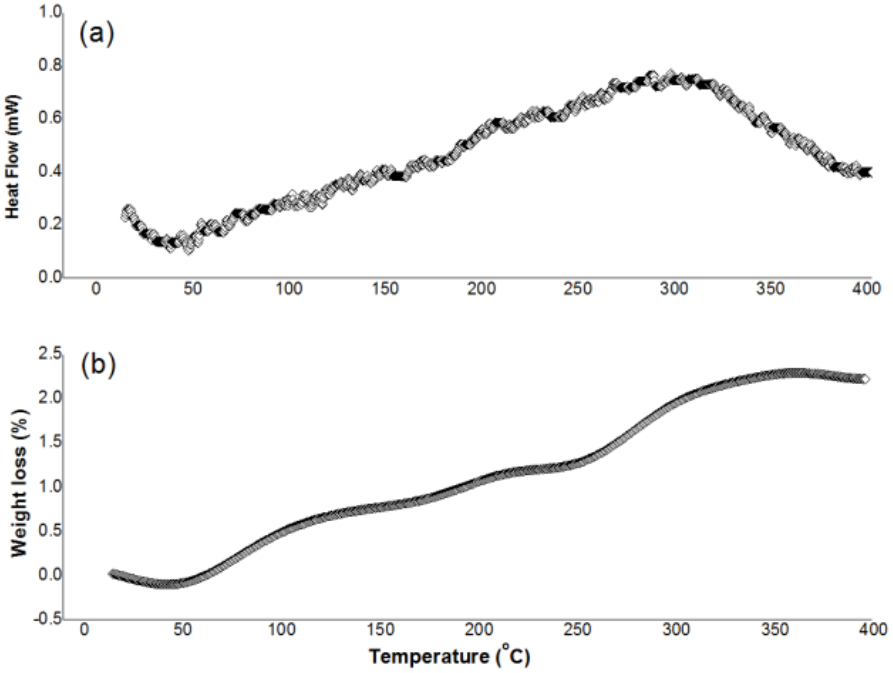

Fig. 5. Thermogravimetric behavior of the Mn_3O_4 precursor during heat-treatment.

surface. As a result of the electrolysis of water molecules, the H_2 molecules are continuously released on the cathode surface during the deposition process, and growth of the H_2 bubbles is occurred so that they can escape from the surface and electrolyte (Fig. 4a). Once the pH at the cathode surface solution reaches a required value, Mn_3O_4 deposits are formed and growth at the cathode surface (Fig. 4b).

Mechanism of Mn_5O_8 formation

To obtain the final oxide product, the prepared deposit was heat treated at 400 °C for 3h as shown in Fig. 4c. The physico-chemical changes during the calcination were investigated by DSC–TG analysis. Fig. 5 shows the DSC-TGA curves of Mn_3O_4 deposit at the temperatures of 25-400 °C. The DSC curve in Fig. 6a has one small endothermic peak at temperatures of 25-150 °C, and a broad exothermic one at temperatures between 150-400 °C. Correspondingly, TG curve exhibits the weight changes for these peaks as clearly seen in

Fig. 5b. The physicochemical changes during the heat changes in DSC curve are as follow:

- The first peak indicates the removal of adsorbed water on the surface of Mn_3O_4 nanorods:

$$[Mn_3O_4 \cdot yH_2O] \rightarrow Mn_3O_4 + yH_2O$$

The TG curve shows a small weigh loss (i.e. 0.19 %) for this step (Fig. 6b). Notably, the trace amount of adsorbed water is due to drying process (60 °C for 1h) on nanorods after deposition process as noted in experimental section. It was reported that the Mn_3O_4 is oxidized to Mn_5O_8 at 300 °C in O_2 atmosphere and then converted to the Mn_2O_3 at temperatures of over 500 °C [14]. Notably, it was also found that Mn_3O_4 phase is directly converted to Mn_2O_3 in air atmosphere at temperatures of over 500 °C [14,34].

- The second peak is due to the conversion of Mn_3O_4 to Mn_5O_8 in the O_2 atmosphere [14]:

$$Mn_3O_4 + 2/5O_2 \rightarrow 3/5Mn_5O_8$$

In fact, in this step oxidation of Mn_3O_4 is occurred in the O_2 atmosphere. This step leads to a weight gain of ~2.39%, which is correspondent with the expected mass gain by complete conversion of Mn_3O_4 to Mn_5O_8 (i.e. 2.8%).

CONCLUSION

Pulse cathodic electrodeposition of Mn oxide was for the first time performed from nitrate bath. The structural investigations by XRD and FT-IR confirmed that Mn_3O_4 deposit have been prepared as the deposition product. Heat-treatment of deposit product was then performed at O_2 atmosphere in 400 oC for 2h. The Mn_5O_8 nanorods were obtained as the calcination product as confirmed by XRD, FT-IR and SEM. In final, the results make pulse deposition as a facile method for preparation of Mn oxide nanoparticles.

CONFLICT OF INTEREST

The author declares that there is no conflict of interests regarding the publication of this manuscript.

REFERENCES

1. Huang S., Wang Y., Wang Z., Zhao K., Shi X., Lai X., Zhang L., (2015), Structural, magnetic and magnetodielectric properties of the Mn_3O_4 thin films epitaxially grown on $SrTiO_3$ (001) substrates. Solid State Commun. 212: 25-29.
2. Sadeghi M., Hosseini M.H., (2012), Preparation and application of MnO_2 nanoparticles/zeolite AgY composite catalyst by confined space synthesis (CSS) method for the desulfurization and elimination of SP and OPP. JNS 2: 441-445.
3. Cai Z., Xu L., Yan M., Han C., He L., Hercule K.M., Niu C., Yuan Z., Xu W., Qu L., Zhao K., Mai L., (2015), Manganese oxide/carbon yolk–shell nanorod anodes for high capacity lithium batteries. Nano Lett. 15: 738–744.
4. Z. Li, Y. Su, G. Yun, K. Shi, X. Lv, B. Yang, (2014), Binder free synthesis of MnO_2 nanoplates/ graphene composites with enhanced supercapacitive properties. Solid State Commun. 192: 82-88.
5. Klingsberg C., Roy R., (1960), Solid-solid and solid-vapor reactions and a new phase in the system Mn-O. J. Am. Ceram. Soc. 43: 620–626.
6. Oswald H.R., Feitknecht W., Wampetich M.J., (1965), Crystal Data of Mn_5O_8 and $Cd_2Mn_3O_8$. Nature 207: 72-72.
7. Oswald H.R., Wampetich M.J., (1967), Die Kristallstrukturen von Mn_5O_8 und $Cd_2Mn_3O_8$. Helv. Chim. Acta 50: 2023–2034.
8. Prinz G.A., (1998), Magnetoelectronics. Science 282: 1660-1663.
9. Wolf S.A., Awschalom D.D., Buhrman R.A., Daughton J.M., Von Molnar S., Roukes M.L., Chtchelkanova A.Y., Treger D.M., (2001), Spintronics: a spin-based electronics vision for the future. Science 294: 1488-1495.
10. Tian Z.R., Tong W., Wang J.Y., Duan N.G., Krishnan V.V., Sui S.L., (1997), Manganese oxide mesoporous structures: mixed-valent semiconducting catalysts. Science 276: 926-930.
11. Gao T., Norby P., Krumeich F., Okamoto H., Nesper R., Fjellvag H., (2010), Synthesis and properties of layered-structured Mn_5O_8 nanorods J. Phys. Chem. C 114: 922–928.
12. Park Y.J., Doeff M.M., (2006), Synthesis and electrochemical characterization of $M_2Mn_3O_8$ (M=Ca, Cu) compounds and derivatives. Solid State Ionics 177: 893–900.
13. Punnoose A., Magnone H., Seehra M.S., (2001), Synthesis and antiferromagnetism of Mn_5O_8 IEEE Transaction on Magnetics 37: 2150-2152.
14. Sugawara M., Ohno M., Matsuki K., (1991) Novel preparation method of manganese(II) manganese(IV) oxide ($Mn_2Mn_3O_8$, Mn_5O_8) by citrate process. Chem. Lett. 1465–1468.
15. Yamamoto N., Kiyama M., Takada T., (1973), A new preparation method of Mn_5O_8. Jpn. J. Appl. Phys. 12 1827–1828.
16. Fritsch S., Sarrias J., Rousset A., Kulkarni G.U., (1998), Low-temperature oxidation of Mn_3O_4 hausmannite. Mater. Res. Bull. 33: 1185–1194.
17. Uddin I., Poddar P., Ahmad A., (2013), Extracellular biosynthesis of water dispersible, protein capped Mn_5O_8 nanoparticles using the fungus fusarium oxysporum and study of their magnetic behavior. J. Nanoeng. Nanomanufact. 3: 91–97.
18. Aghazadeh M., Barmi A.A.M., Gharailou D., Peyrovi M.H., Sabour B., (2013), Cobalt hydroxide ultra-fine nanoparticles with excellent energy storage ability. Appl. Surf. Sci. 283: 871-875.
19. Barani A., Aghazadeh M., Ganjali M.R., Sabour B., Barmi A.A.M., Dalvand S., (2014), Nanostructured nickel oxide ultrafine nanoparticles: synthesis, characterization, and supercapacitive behavior. Mater. Sci. Semiconduct. Process. 23 85-92.
20. Aghazadeh M., Barmi A.A.M., Hosseinifard M., (2012), Nanoparticulates $Zr(OH)_4$ and ZrO_2 prepared by low-temperature cathodic electrodeposition. Mater. Lett. 73: 28-31.
21. Aghazadeh M., Hosseinifard M., (2013), Electrochemical

preparation of ZrO_2 nanopowder: impact of the pulse current on the crystal structure, composition and morphology. Ceram. Int. 39: 4427-4435.
22. Aghazadeh M., Yousefi T., Ghaemi M., (2012), Electrochemical preparation and characterization of brain-like nanostructures of Y_2O_3. J. Rare Earths 30: 236-240
23. Aghazadeh M., Maragheh M.G., Ganjali M.R., Norouzi P., Faridbod F., (2016), Electrochemical preparation of MnO_2 nanobelts through pulse base-electrogeneration and evaluation of their electrochemical performance. Appl. Surf. Sci. 364: 141-147.
24. Aghazadeh M., Ahmadi R., Gharailou D., Ganjali M.R., Norouzi P., (2016), Electrochemical preparation and supercapacitive performance of α-MnO_2 nanospheres with secondary wall-like structures. J. Mater. Sci.: Mater. Electron. DOI 10.1007/s10854-016-4882-x.
25. Davar F., Salavati-Niasari M., Mir N., Saberyan K., Monemzadeh M., Ahmadi E., (2010), Thermal decomposition route for synthesis of Mn_3O_4 nanoparticles in presence of a novel precursor. Polyhedron 29: 1747-1753.
26. Koza J.A., Schroen I.P., Willmering M.M., Switzer J.A., (2014), Electrochemical synthesis and nonvolatile resistance switching of Mn_3O_4 thin films. Chem. Mater. 26: 4425-4432.
27. Yousefi T., Nozad Golikand A., Mashhadizadeh M.H., Aghazadeh M., (2012), Hausmannite nanorods prepared by electrodeposition from nitrate medium via electrogeneration of base. J. Taiwan Inst. Chem. Eng. 43: 614-618.
28. Ishii M., Nakahira M., Yamanaka T., (1972), Infrared absorption spectra and cation distributions in (Mn, $Fe)_3O_4$. Solid State Commun. 11: 209–212.
29. Wang W.Z., Xu C.K., Wang G.H., Liu Y.K., Zheng C.L., (2002), Preparation of smooth single-crystal Mn_3O_4 nanowires. Adv. Mater. 14: 837-840.
30. Gupta N., Verma A., Kashyap S.C., Dube D.C., (2007), Microstructural, dielectric and magnetic behavior of spindeposited nanocrystalline nickel-zinc ferrite thin films for microwave applications. J. Magn. Magnet. Mater. 308: 137-142.
31. Azzoni C.B., Mozzati M.C., Galinetto P., Paleari A., Massarotti V., Capsoni D., Bini M., (1999), Thermal stability and structural transition of metastable Mn_5O_8. Solid State. Commun. 112: 375–378.
32. Khosrow-pour F., Aghazadeh M., Arhami B., (2013), Facile synthesis of vertically aligned one-dimensional (1D) $La(OH)_3$ and La_2O_3 nanorods by pulse current deposition. J. Electrochem. Soc. 160: D150-D155.
33. Aghazadeh M., Ghaemi M., Golikand A.N., Ahmadi A., (2011), Porous network of Y_2O_3 nanorods prepared by electrogeneration of base in chloride medium. Mater. Lett. 65: 2545-2548.